

# STOCHASTIC OPTIMAL PREDICTION FOR THE KURAMOTO-SIVASHINSKY EQUATION \*

PANAGIOTIS STINIS<sup>†</sup>

**Abstract.** We examine the problem of predicting the evolution of solutions of the Kuramoto-Sivashinsky equation when initial data are missing. We use the optimal prediction method to construct equations for the reduced system. The resulting equations for the resolved components of the solution are random integrodifferential equations. The accuracy of the predictions depends on the type of projection used in the integral term of the optimal prediction equations and on the choice of resolved components. The novel features of our work include the first application of the optimal prediction formalism to a nonlinear, non-Hamiltonian equation and the use of a non-invariant measure constructed through inference from empirical data.

**Key words.** Optimal prediction, Memory, Orthogonal dynamics, Underresolution, Hermite polynomials, Kuramoto-Sivashinsky equation

**AMS subject classifications.** 65C20,82C31

**1. Introduction.** Computer applications to science and engineering continue to expand. However, there is still a wealth of problems where the computational power we can bring to bear is not sufficient and thus the calculations we perform are underresolved. This situation leads to a twofold question: What quantities should one strive to predict and what are the equations that describe the evolution of these quantities?

The purpose of this work is to examine the problem of prediction in the presence of underresolution for the Kuramoto-Sivashinsky equation which models pattern formation in different physical contexts [21, 34]. We will be using the equation in the form

$$v_t + \nu v_x + v_{xx} + \nu v_{xxxx} = 0, \quad (1.1)$$

in the domain  $[0, 2\pi]$  with periodic boundary conditions and initial condition  $v_0(x)$ . The parameter  $\nu$  has the conventional interpretation of viscosity and controls the rate of energy dissipation at the small scales. Depending on the value of the parameter  $\nu$  the solutions can exhibit a wide range of behavior, from steady states, to periodic solutions in time, to solutions with coherent spatial structures that evolve chaotically in time (such solutions will be called chaotic), to solutions that exhibit temporal chaoticity together with long range spatial statistical independence (spatio-temporal chaos) [4, 12, 19]. The problem of modelling the behavior of the Kuramoto-Sivashinsky equation using a reduced set of variables has proved to be a formidable one and different tools have been used towards this goal [40, 36, 33, 38].

We are addressing the problem of underresolved computations through the method of optimal prediction [9, 10]. In order to proceed in the formulation of the equations for the quantities that will be predicted it is necessary to have some knowledge about the degrees of freedom that are unresolved. In optimal prediction what is assumed

---

\*This work was supported in part by the Applied Mathematical Sciences subprogram of the Office of Energy Research of the US Department of Energy under Contract DE-AC03-76-SF00098, in part by the National Science Foundation under Grant DMS98-14631 and in part by the Columbia University Boris A. Bakhmeteff Research Fellowship in Fluid Mechanics.

<sup>†</sup>Department of Applied Physics and Applied Mathematics, Columbia University, New York, NY 10027 (stinis@math.lbl.gov).

as known is an initial measure on the space of solutions. What is sought is a mean solution with respect to this initial measure, compatible with the partial information available initially as well as with the limitations on the available computing power. This mean solution is the conditional expectation of the solution given the partial initial data, and is the best available estimate of the solution of the full problem. The optimal prediction method consists of ways to construct equations that will allow the calculation of the conditional expectation of the solution.

We are looking at a Galerkin Fourier truncation of the Kuramoto-Sivashinsky equation, thus, the solution of the equation is determined through the integration in time of a system of ordinary differential equations for the Fourier modes. The resolved variables will be a set of Fourier modes, smaller than what is needed for a full description of the system. The goal is to produce estimates for the evolution of the conditional expectations of the resolved Fourier modes conditioned on their prescribed initial values.

The first step towards this goal is to compute the true conditional expectations (what will be later called the truth). To do that requires the knowledge of a measure on the space of all the Fourier modes (resolved and unresolved). The Kuramoto-Sivashinsky equation has no natural candidate for this measure. We evolve repeatedly, using initial conditions drawn from a uniform distribution, the equations needed for the full description of the system and collect the values of all the Fourier modes after some prescribed time interval. In this way we obtain a collection of samples of the values of the Fourier modes. We, then, use maximum likelihood estimation to construct an approximation to the measure that describes the distribution of these samples. We construct a diagonal Gaussian approximation to the measure (the reason for the use of a diagonal measure is given later). The reason that we choose a Gaussian measure is that, inspection of the first few moments of the collection of samples, reveals that some of the modes have Gaussian statistics. Our future plan is to construct more elaborate approximations to the measure (e.g. mixtures of diagonal Gaussian measures using the Expectation-Maximization algorithm [28]). The measure constructed is sampled, keeping the resolved Fourier modes fixed to their prescribed values. We use the samples as initial conditions to integrate the equations for all the Fourier modes. The true conditional expectations of the resolved modes given their initial values, are the averages of the resolved modes over the samples.

The second step is to produce estimates for these conditional expectations. To do that we need to construct equations for the evolution of the resolved modes. This is achieved through the use of the optimal prediction formalism that utilizes the measure constructed through maximum likelihood estimation. We use the optimal prediction formalism in a certain limit called the short-memory approximation. This approximation is valid if the resolved modes depend only on their recent history. The short-memory approximation is more general than the delta-function approximation used frequently in the statistical physics literature, where the resolved modes' evolution is assumed to depend only on their present values. In fact, the delta-function approximation can be derived as a limiting case of the short-memory approximation.

The optimal prediction equations for the resolved modes, in the short-memory approximation, are random ordinary integrodifferential equations. They contain a Markovian term, depending only on the resolved modes' current values, a memory term that depends on the recent values of the resolved modes and a random term that depends on the unresolved modes. The optimal prediction equations are solved repeatedly for different realizations of their random part. The initial conditions for

the resolved modes are the same for all realizations. The estimates of the conditional expectations of the resolved modes given their initial values are the averages, over the different realizations, of the values of these modes. We compare the estimates produced in this way to the true conditional expectations. The results depend on the set of variables that are resolved and on the type of projection used in the memory term. If the set of resolved variables includes all the linearly unstable modes and the projection of the memory term is on the span of the resolved modes (linear projection), the agreement between the estimates of the conditional expectations and the true conditional expectations is good for relatively long times. If the set of resolved variables includes all the linearly unstable modes and the projection of the memory term is on an orthonormal set of functions of the resolved modes (finite-rank projection), the agreement between the estimates of the conditional expectations and the true conditional expectations is good for short times only. If, even one linearly unstable mode is left unresolved, the agreement between the estimates and the true conditional expectations is good for short times only.

**2. Optimal prediction formalism and the short-memory approximation.** We present the optimal prediction formalism in full generality and derive from it the approximation that we will be using later, namely the short-memory approximation.

**2.1. Conditional expectations and the Mori-Zwanzig formalism.** Suppose we are given a system of ordinary differential equations

$$\frac{d\phi}{dt} = R(\phi)$$

with initial condition  $\phi(0) = x$ , and we know only a fraction of the initial data, say  $\hat{x}$ , where  $x = (\hat{x}, \tilde{x})$  and correspondingly  $\phi = (\hat{\phi}, \tilde{\phi})$  and that the unresolved data are drawn from a measure with density  $f(x)$  (we will be working only with measures that are smooth enough to have a density).

Suppose  $u, v$  are functions of  $x$ , and introduce the scalar product  $(u, v) = E[uv] = \int u(x)v(x)f(x)dx$ . We will denote the space of functions  $u$  with  $E[u^2] < \infty$  by  $L_2(f)$  or simply  $L_2$ . We are looking for approximations of functions of  $x$  by functions of  $\hat{x}$ , where  $\hat{x}$  are the variables that form our reduced system (the resolved degrees of freedom). The functions of  $\hat{x}$  form a closed linear subspace of  $L_2$ , which we denote by  $\hat{L}_2$ . Given a function  $u$  in  $L_2$ , its conditional expectation with respect to  $\hat{x}$  is

$$E[u|\hat{x}] = \frac{\int u f d\tilde{x}}{\int f d\tilde{x}}.$$

The conditional expectation  $E[u|\hat{x}]$  has the following properties:

- $E[u|\hat{x}]$  is a function of  $\hat{x}$ ,
- $E[au + bv|\hat{x}] = aE[u|\hat{x}] + bE[v|\hat{x}]$ ,
- $E[u|\hat{x}]$  is the best approximation of  $u$  by a function of  $\hat{x}$ :

$$E[|u - E[u|\hat{x}]|^2] \leq E[|u - h(\hat{x})|^2]$$

for all functions  $h$ .

We can approximate the conditional expectation  $E[u|\hat{x}]$  by picking a basis in  $\hat{L}_2$ , for example  $h_1(\hat{x}), h_2(\hat{x}), \dots$ . For simplicity assume that the basis functions  $h_i(\hat{x})$  are orthonormal, i.e.,  $E[h_i h_j] = \delta_{ij}$ . The approximation of the conditional expectation

can be written as  $E[u|\hat{x}] = \sum a_j h_j(\hat{x})$ , where  $a_j = E[uh_j] = E[u(\hat{x}, \tilde{x})h_j(\hat{x})]$ . If we have a finite number of terms only, we are projecting on a smaller subspace and the projection is called a finite-rank projection. In the special case where we pick as basis functions in  $\hat{L}_2$  the functions  $h_1(\hat{x}) = x_1, h_2(\hat{x}) = x_2, \dots, h_m(\hat{x}) = x_m$ , then the corresponding finite-rank projection is called in physics the "linear" projection (note that all projections are linear, so "linear" is used to denote that the projection is on linear functions of the resolved variables). We should note here that it is not always true that  $E[x_i x_j] = 0$  for  $i \neq j$ .

The system of ordinary differential equations we are asked to solve can be transformed into the linear partial differential equation [8]

$$u_t = Lu, \quad u(x, 0) = g(x) \quad (2.1)$$

where  $L = \sum_i R_i(x) \frac{\partial}{\partial x_i}$  is the Liouvillian and the solution of (2.1) is given by  $u(x, t) = g(\phi(x, t))$ . Consider the following initial condition for the PDE

$$g(x) = x_j \Rightarrow u(x, t) = \phi_j(x, t)$$

We can rewrite the solution symbolically as

$$u(x, t) = e^{tL} x_j$$

This implies that for the general case where  $u(x, 0) = g(x)$ , the solution is

$$u(x, t) = e^{tL} g(x) = g(e^{tL} x).$$

Using the symbolic representation we can rewrite (2.1) as

$$\frac{\partial}{\partial t} e^{tL} x_j = L e^{tL} x_j$$

and furthermore by using the identity  $L e^{tL} = e^{tL} L$  (2.1) becomes

$$\frac{\partial}{\partial t} e^{tL} x_j = e^{tL} L x_j. \quad (2.2)$$

If  $P$  is any of the projections mentioned before and  $Q = I - P$ , (2.2) can be rewritten as [8]

$$\frac{\partial}{\partial t} e^{tL} x_j = e^{tL} P L x_j + e^{tQL} Q L x_j + \int_0^t e^{(t-s)L} P L e^{sQL} Q L x_j ds, \quad (2.3)$$

where we have used Dyson's formula

$$e^{tL} = e^{tQL} + \int_0^t e^{(t-s)L} P L e^{sQL} ds. \quad (2.4)$$

Equation (2.3) is the Mori-Zwanzig identity [41, 30, 29]. Note that this relation is exact and is an alternative way of writing the original PDE. It is the starting point of our approximations. Of course, we have one such equation for each of the resolved variables  $\phi_j, j = 1, \dots, m$ . The first term in (2.3) is usually called Markovian since it depends only on the values of the variables at the current instant, the second is called "noise" and the third "memory". The meaning of the different terms appearing in

(2.3) and a connection (and generalization) to the fluctuation-dissipation theorems of irreversible statistical mechanics can be found in [9, 35].

If we write

$$e^{tQL}QLx_j = w_j,$$

$w_j(x, t)$  satisfies the equation

$$\begin{cases} \frac{\partial}{\partial t}w_j(x, t) = QLw_j(x, t) \\ w_j(x, 0) = QLx_j = R_j(x) - \mathfrak{R}_j(\hat{x}). \end{cases} \quad (2.5)$$

If we project (2.5) using any of the projections discussed we get

$$P\frac{\partial}{\partial t}w_j(x, t) = PQLw_j(x, t) = 0,$$

since  $PQ = 0$ . Also for the initial condition

$$Pw_j(x, 0) = PQLx_j = 0$$

by the same argument. Thus, the solution of (2.5) is at all times orthogonal to the space of functions of  $\hat{x}$ . We call (2.5) the orthogonal dynamics equation.

**2.2. The short-time and short-memory approximations.** The approximation we will examine is a short-time approximation and consists of dropping the integral term in Dyson's formula (2.4)

$$e^{tQL} \cong e^{tL}. \quad (2.6)$$

In other words we replace the flow in the orthogonal complement of  $\hat{L}_2$  with the flow induced by the full system operator  $L$ . Some algebra shows that

$$Q(e^{sQL} - e^{sL}) = O(s^2), \quad (2.7)$$

and

$$\int_0^t e^{(t-s)L}PLE^{sQL}QLx_j ds = \int_0^t e^{(t-s)L}PLQe^{sL}QLx_j ds + O(t^3). \quad (2.8)$$

As expected dropping the integral term in Dyson's formula yields an approximation that is good only for short times. However, under certain conditions this approximation can become valid for longer times. To see that consider the case where  $P$  is the finite-rank projection so

$$PLQe^{sQL}QLx_j = \sum_{k=1}^l (LQe^{sQL}QLx_j, h_k)h_k(\hat{x}), \quad (2.9)$$

and for the approximation

$$PLQe^{sL}QLx_j = \sum_{k=1}^l (LQe^{sL}QLx_j, h_k)h_k(\hat{x}). \quad (2.10)$$

The quantities  $(LQe^{sL}QLx_j, h_k)$  can be calculated from the full system without recourse to the orthogonal dynamics. Recall (2.7) which states that the error in approximating  $e^{sQL}$  by  $e^{sL}$  is small for small  $s$ . This means that for short times we can infer the behavior of the quantity  $(LQe^{sQL}QLx_j, h_k)$  by examining the behavior of the quantity  $(LQe^{sL}QLx_j, h_k)$ .

If the quantities  $(LQe^{sL}QLx_j, h_k)$  decay fast we can infer that the quantities  $(LQe^{sQL}QLx_j, h_k)$  decay fast for short times. We cannot infer anything about the behavior of  $(LQe^{sQL}QLx_j, h_k)$  for larger times. However, if  $(LQe^{sQL}QLx_j, h_k)$  not only decay fast initially, but, also, stay small for larger times, then we expect our approximation to be valid for larger times. To see this consider again the integral term in the Mori-Zwanzig equation. We see that the integral does not extend from 0 to  $t$  but only from  $t - t_0$  to  $t$ , where  $t_0$  is the time of decay of the quantities  $(LQe^{sQL}QLx_j, h_k)$ . This means that our approximation becomes

$$\begin{aligned} \int_0^t e^{(t-s)L} P L e^{sQL} Q L x_j ds &\cong \int_{t-t_0}^t e^{(t-s)L} P L Q e^{sQL} Q L x_j ds \\ &= \int_{t-t_0}^t e^{(t-s)L} P L Q e^{sL} Q L x_j ds + \int_{t-t_0}^t O(s^2) ds \\ &= \int_{t-t_0}^t e^{(t-s)L} P L Q e^{sL} Q L x_j ds + O(t^2 t_0). \end{aligned} \quad (2.11)$$

From this we conclude that the short-time approximation is valid for large times if  $t_0$  is small and is called the short-memory approximation. On the other hand, if  $t_0$  is large, then the error is  $O(t^3)$  and the approximation is only valid for short times. Note that the validity of the short-memory approximation can only be checked after constructing it, since it is based on an assumption about the large time behavior of the unknown quantities  $(LQe^{sQL}QLx_j, h_k)$ . Note, that determination of the quantities  $(LQe^{sQL}QLx_j, h_k)$  requires the (usually very expensive) solution of the orthogonal dynamics equation. The short-memory approximation, when valid, allows us to avoid the solution of the orthogonal dynamics equation.

If the quantities  $(LQe^{sL}QLx_j, h_k)$  do not decay fast, then we can infer, again only for short times, that the quantities  $(LQe^{sQL}QLx_j, h_k)$  of the exact Mori-Zwanzig equation do not decay fast. Yet, it is possible that the quantities  $(LQe^{sQL}QLx_j, h_k)$  start decaying very fast after short times and remain small for longer times, so that the short-memory approximation could still hold. Of course, this can only be checked a posteriori, after the simulation of the short-memory approximation equations.

In the statistical physics literature, the assumption that the correlations vanish for  $s \neq 0$  is often made which is a special case of the short-memory approximation with the correlations replaced by a delta-function multiplied by the integrals. We shall also comment on this drastic approximation for our problem later when we present the numerical simulations of the short-memory approximation equations. An application of the short-memory approximation can be found in [1].

**3. Density estimation.** Since the Kuramoto-Sivashinsky (KS) equation does not have a natural candidate for the measure on the space of solutions, we have to construct an approximation to this measure. We do so by means of maximum likelihood estimation. To find the maximum likelihood estimate of the parameters of the measure approximation we need to obtain samples of the solution of the equation. This is accomplished through the numerical solution of the equation for different

initial conditions sampled from a uniform distribution on the space of solutions. The measure constructed through maximum likelihood estimation is used later to compute the optimal prediction equations.

**3.1. Numerical solution of the KS equation.** As mentioned earlier, we are looking at a Fourier-Galerkin truncation of the solution. We expand the solution in Fourier series and retain the first  $N$  terms,

$$v_N = \sum_{k=-\frac{N}{2}}^{\frac{N}{2}-1} u_k(t) e^{ikx},$$

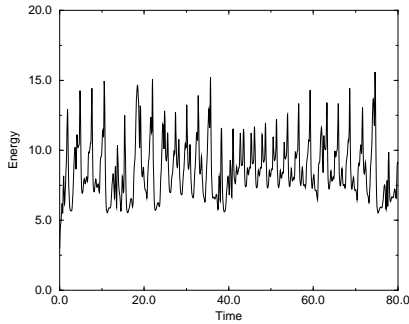
where  $u_k(t)$  are the time-dependent Fourier coefficients. The asymmetry between positive and negative wavenumbers comes from the fact that we will be working with an even number of modes. Since the solution of KS is real,  $u_{-k} = u_k^*$ , where, as before,  $*$  denotes complex conjugation. The Fourier expansion transforms (1.1) into a system of ordinary differential equations (ODE) which reads

$$\frac{du_k}{dt} = -\frac{ik}{2} \sum_{k'=-\frac{N}{2}}^{\frac{N}{2}-1} u_{k'} u_{k-k'} + (k^2 - \nu k^4) u_k. \quad (3.1)$$

The KS equation conserves the mean value  $\frac{1}{2\pi} \int_0^{2\pi} v(x) dx = u_0$ . In all subsequent calculations we assume  $u_0 = 0$  without loss of generality. Linear stability analysis shows that the rate of growth for the mode  $k$  is  $k^2 - \nu k^4$ . This makes the first  $\lfloor \nu^{-\frac{1}{2}} \rfloor$  (where  $\lfloor \cdot \rfloor$  stands for the integer part) modes linearly unstable. The mode  $\lfloor (2\nu)^{-\frac{1}{2}} \rfloor$  is the most unstable. Because of the presence of the fourth order stabilizing term, the stable modes have decay rates that increase rapidly with increasing wavenumber thus making the system stiff (see [22] for an extended discussion of stiffness). The presence of the nonlinear coupling does not alter the stiffness of the ODE system. It is this property precisely that dictates the need for (i) an implicit solver that guarantees stability and (ii) a solver with variable step size to control the errors.

The method we chose for our numerical experiments is a variable-step variable-order multistep method based on the Backward Differentiation Formulas (BDF) that employs the Nordsieck representation for the storing of the necessary quantities at each instant [16, 14]. The BDF methods are implicit multistep methods that, up to order 6, are stable. Since the method of integration is implicit it results in a system of nonlinear algebraic equations that has to be solved iteratively and we do that by the Newton-Raphson method. Finally, the convolution sums in the RHS of the equations are evaluated in real space using an FFT transform and the 3/2 rule for dealiasing [6]. Because we are using an even number of modes the mode  $-\frac{N}{2}$  is set equal to zero to ensure that the solution to KS is a real function.

All our calculations were performed with the value of the viscosity  $\nu = 0.085$ . This value was chosen because it belongs in the first window that supports chaotic solutions. The first 3 Fourier modes are linearly unstable and mode  $k = 2$  is the most unstable linearly. As suggested by the numerical simulations, the energy spectrum shows a pronounced peak at this mode. Experiments with different number of modes show that for  $N \geq 24$  the solution is converged for the time interval that we are interested in. For the experiments, an error tolerance of  $10^{-7}$  per step was chosen.



(a)

FIG. 3.1. Evolution of the energy  $E = \frac{1}{4\pi} \int_0^{2\pi} v_N^2(x, t) dx$ .

Simulations with stricter error tolerances up to  $10^{-10}$  did not show any change in the behavior of the solutions, so we kept the value of  $10^{-7}$  which allows for faster calculations. Strict tolerance criteria are dictated by the well-documented extreme sensitivity of the KS system to small errors [18, 19]. If high accuracy is not enforced it is possible, for some values of the viscosity that actually support chaotic solutions, to observe convergence to a steady state. On Fig.(3.1) we show the evolution of the  $L_2$  norm  $E = \frac{1}{4\pi} \int_0^{2\pi} v_N^2(x, t) dx$  for a typical solution at this value of the viscosity. We denote the  $L_2$  norm by  $E$  and call it the energy of the system. To compute the maximum likelihood estimate we need to obtain a number of independent samples of the solution. This was done by starting the simulation from different random initial conditions, evolving up to time  $t = 5$  and then recording the values of the Fourier modes. The time  $t = 5$  was chosen on the basis of the statistics of the collected samples. These statistics resemble the behavior found in the literature [38] for long-time asymptotics. The random initial conditions were picked uniformly in the range  $[-1, 1]$  for all Fourier modes. We collected 10000 independent samples of the solution, and it is these samples that we used in the calculation of the maximum likelihood estimate.

**3.2. Maximum likelihood estimation.** Let  $\mathbf{w}_1, \mathbf{w}_2, \dots, \mathbf{w}_n$  denote  $n$  independent samples of a random  $d$ -dimensional vector  $\mathbf{W}$  with probability density function (p.d.f.)  $f(\mathbf{w}, \Psi)$  where  $\Psi$  is the vector of parameters that determine the p.d.f.. Let

$$\mathbf{y} = (\mathbf{w}_1^T, \dots, \mathbf{w}_n^T)^T.$$

If we define the probability density  $g(\mathbf{y}, \Psi)$  as

$$g(\mathbf{y}, \Psi) = \prod_{j=1}^n f(\mathbf{w}_j, \Psi),$$

then the likelihood function formed from the observed data  $\mathbf{y}$  is defined by

$$L(\Psi) = g(\mathbf{y}, \Psi).$$



The vector  $\Psi$  is to be estimated by maximizing the likelihood [23]. An estimate  $\hat{\Psi}$  of  $\Psi$  can be obtained as a solution of the likelihood equation  $\frac{\partial L(\Psi)}{\partial \Psi} = 0$ , or equivalently,  $\frac{\partial \log L(\Psi)}{\partial \Psi} = 0$ .

Our initial aim was to approximate the density on the space of the Fourier modes by a mixture of Gaussian densities. Application of the maximum likelihood method to obtain  $\Psi$ , results in equations that cannot be solved in closed form. However, this problem can be tackled by the application of iterative procedures like the Expectation-Maximization (EM) algorithm [28]. But the application of the EM algorithm in such a high dimensional setting as the one we have is not straightforward. Two problems appear [31]: The first is the problem of "overfitting", where a small cluster of points, or even worse, a single point, determine the properties of one of the components, thus making the entries of the covariance matrix of the component acquire very small values that, in their turn, create numerical problems with the numerical implementation of the algorithm (we call such a component "narrow"). The second problem comes from the fact that, if the likelihood function has multiple maxima, the EM algorithm is only guaranteed to converge to a local maximum that depends on the initial values used for the parameters. This restricts the ability of the computed mixture to be applied to the estimation of the density of new data points.

The KS equation is stiff and this creates an extra difficulty because the most stable modes of the system have very small variances. The normalization constant of a Gaussian  $((4\pi)^d |A|)^{-1} \exp[-\frac{1}{2}(\mathbf{w} - \mu)^* A^{-1}(\mathbf{w} - \mu)]$  for  $d$  complex variables is  $(4\pi)^d |A|$ , where  $|A| = \prod_{i=1}^d (4\pi \lambda_i)$  and  $\lambda_1, \dots, \lambda_d$  are the eigenvalues of  $A$ . The very small variances for the most stable modes result in very small values for the corresponding eigenvalues, which in their turn make the normalization constant acquire very small values. This creates, again, problems with the numerical implementation (see [35]), since we have to deal with a "narrow" component as above. But, more importantly, it becomes increasingly difficult to decide, if a "narrow" component appears, whether it stems from overfitting or it should be there to describe the KS statistics.

Different methods have been proposed to deal with the problems of overfitting and convergence to only local maxima for general Gaussian mixtures [32, 3, 37]. We shall adopt here a more modest goal and try to approximate the density with only one Gaussian. Of course, for the case of only one Gaussian component, we can compute the properties of the Gaussian by direct maximization of the likelihood function. However, our future goal is to use a mixture of Gaussian components to describe more accurately the density of the Fourier modes.

Before we estimate the parameters of the Gaussian density we make an additional simplification dictated by the statistical properties of the collected samples. The covariance matrix for the Fourier modes based on the collected samples is

$$Cov[w_i, w_j^*] = \frac{1}{n-1} \sum_{k=1}^n (w_{ki} - M_i)(w_{kj} - M_j)^*,$$

for  $i, j = 1, \dots, d$  where  $M_i, i = 1, \dots, d$  are the means  $M_i = \frac{1}{n} \sum_{k=1}^n w_{ki}$ . Our numerical experiments indicate that the covariance matrix for the KS system is almost diagonal, i.e. the non-diagonal entries are very small compared to the diagonal ones (results from [24] also support this conclusion). We discard the off-diagonal elements and work with a Gaussian density with a diagonal matrix.

The fact that the solution of the KS equation is real induces a constraint on the values of the Fourier modes, namely for each wavenumber  $k$  we have,  $u_{-k} = u_k^*$ .

We can incorporate the constraint for the Fourier modes in the expression for the Gaussian density. If we order the Fourier modes so that the first  $\frac{d}{2}$  positions of the vector  $\mathbf{w}$  of modes are occupied by the modes with positive wavenumbers  $1, \dots, \frac{d}{2}$  and the rest  $\frac{d}{2}$  positions by the modes with negative wavenumbers  $-1, \dots, -\frac{d}{2}$ , we can write the Gaussian density (with the constraint) as

$$Z^{-1} \exp\left[-\frac{1}{2}(\mathbf{w} - \boldsymbol{\mu})^* A^{-1}(\mathbf{w} - \boldsymbol{\mu})\right] \prod_{i=1}^{\frac{d}{2}} \delta(w_{i+\frac{d}{2}} - w_i^*), \quad (3.2)$$

where  $A = \text{diag}(a_1, \dots, a_d)$ . The entries of the matrix  $A$  have the property  $a_{i+\frac{d}{2}} = a_i$  for  $i = 1, \dots, \frac{d}{2}$ , since they are the variances of the modes  $u_i$  and  $u_{i+\frac{d}{2}}$  which according to our ordering are complex conjugates of each other. Also,  $\mu_{i+\frac{d}{2}} = \mu_i^*$  for  $i = 1, \dots, \frac{d}{2}$ .

The normalization constant  $Z$  (modified due to the constraint) is  $Z = \prod_{i=1}^{\frac{d}{2}} (2\pi a_i)$ .

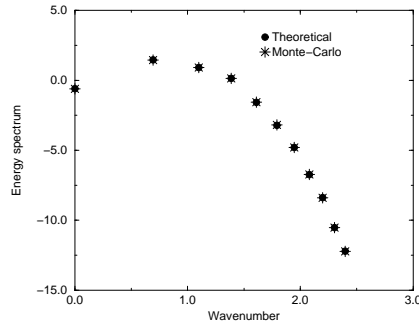
The numerical results of the simulations for the KS equation are converged with  $N = 24$  modes. However, because the zero mode (i.e. the mean value of the real-space solution) is constant and taken equal to zero and the  $-\frac{N}{2}$ th mode was set equal to zero as explained above, the effective number of modes is  $\bar{N} = 22$ . Thus the dimension  $d$  for the Gaussian density is 22. The formulas for the estimation of the parameters of the Gaussian density are

$$\mu_i = \frac{1}{n} \sum_{j=1}^n w_{ji}, \quad (3.3)$$

$$A_{ii} = \frac{1}{n} \sum_{j=1}^n (w_{ji} - \mu_i)(w_{ji} - \mu_i)^*, \quad (3.4)$$

for  $i = 1, \dots, d$ . In order to check how well the Gaussian describes the statistics of the collection of samples, we computed the first 4 moments (mean, covariance, skewness and flatness) of the samples. The Gaussian density determined by maximum likelihood reproduces very accurately the first three moments of the samples. The third moment of a Gaussian density is identically zero and thus it means that the distribution of a Fourier mode is symmetric around its mean value. The KS dynamics become evident in the fourth moment. The 4th order experimental statistics show a strong deviation from Gaussianity that manifests itself as negative flatness for the most unstable modes and positive flatness for the most stable modes. A negative flatness for the most unstable modes suggests the existence of large weights for values close to the mean value. Such large weights in the p.d.f. of the most unstable modes have been related ([38]) to the appearance of coherent structures at these scales. On the other hand, a positive flatness for the most stable modes suggests the existence of large weights at the tails of the p.d.f.. They have been related to the appearance of rare bursts of activity at these scales. These rare bursts of activity are the space-time defects (creation and annihilation of basic cell-structures) mentioned earlier.

The fact that a single Gaussian density cannot model accurately all the moments means that this density is not invariant for the equation. This will result in a complication for the formulas of the optimal prediction equations. If the density was invariant and we used the finite-rank projection we could have a fluctuation-dissipation relation [35] which would yield significantly simpler expressions for certain terms of the optimal prediction equations.



(a)

FIG. 3.2. Log-log plot of the variances for different Fourier modes as computed by 10000 Monte-Carlo samples and as predicted by the Gaussian density.

The Gaussian density constructed through maximum likelihood can be sampled via Monte-Carlo [2], or by producing independent samples of Gaussian distributions of the appropriate variance for each of the Fourier modes (e.g. using the Box-Mueller algorithm) [20]. The results can be seen in Fig.(3.2).

**4. Optimal prediction for Kuramoto-Sivashinsky.** We proceed to construct the short-memory approximation optimal prediction equations for KS. To conform with the optimal prediction formalism we set

$$R_k(\mathbf{u}) = -\frac{ik}{2} \sum_{k'=-\frac{N}{2}}^{\frac{N}{2}-1} u_{k'} u_{k-k'} + (k^2 - \nu k^4) u_k$$

and we get

$$\frac{du_k}{dt} = R_k(\mathbf{u}) \quad (4.1)$$

for  $k = -\frac{N}{2}, \dots, \frac{N}{2} - 1$ . The system of equations is supplemented with the initial condition  $\mathbf{u}(0) = \mathbf{u}_0$ . The initial condition can be written as  $\mathbf{u}_0 = (\hat{\mathbf{u}}_0, \tilde{\mathbf{u}}_0)$ , where  $\hat{\mathbf{u}}_0$  is the vector of resolved variables and  $\tilde{\mathbf{u}}_0$  the vector of unresolved ones. Recall, that the KS equation conserves the zero mode  $u_0$  which we have set to zero for our numerical experiments. Also, the  $-\frac{N}{2}$ th mode is set to zero to preserve the reality of the solution of KS. This makes the effective number of modes for the truncation equal to  $N - 2$ . This  $(N - 2)$ -dimensional vector is the vector of all the modes, resolved and unresolved. We set  $n = N - 2$  to conform with the optimal prediction formalism. In what follows we will refer to the system of  $n$  Fourier modes as the full system. The vector of resolved variables will be a subset of the  $n$ -dimensional vector of Fourier modes containing  $m$  modes. The unresolved modes are the rest  $n - m$  modes. The  $m$ -dimensional vector of resolved modes contains  $\frac{m}{2}$  positive wavenumber modes and their corresponding  $\frac{m}{2}$  negative wavenumber modes. Accordingly, the vector of unresolved modes contains  $\frac{n-m}{2}$  positive wavenumber modes and their corresponding  $\frac{n-m}{2}$  negative wavenumber modes. We do not specify which Fourier modes will be resolved since in our numerical experiments we use different sets of Fourier modes

as resolved. By relabeling the resolved Fourier modes we can order them from 1 to  $m$  and thus we can construct the optimal prediction equations without any explicit reference to the set of resolved modes.

The equations for the evolution of the set of  $m$  resolved variables in the short-memory approximation are

$$\frac{\partial}{\partial t} e^{tL} u_{0j} = e^{tL} PLu_{0j} + e^{tL} QLu_{0j} + \int_0^t e^{(t-s)L} PLQe^{sL} QLu_{0j} ds, \quad (4.2)$$

where  $j = 1, \dots, m$ ,  $L = \sum_{i=1}^n R_i(\mathbf{u}_0) \frac{\partial}{\partial u_{0i}}$  and  $u_{0j} = u_j(0)$ . Since  $PLu_{0j} = \mathfrak{R}_j(\hat{\mathbf{u}}_0)$ ,  $Lu_{0j} = R_j(\mathbf{u}_0)$  we have

$$QLu_{0j} = R_j(\mathbf{u}_0) - \mathfrak{R}_j(\hat{\mathbf{u}}_0). \quad (4.3)$$

**4.1. Markovian term.** We proceed with the calculation of the first term  $PLu_{0j} = \mathfrak{R}_j(\hat{\mathbf{u}}_0)$  in (4.2). For the case of a Gaussian density the conditional expectations can be computed explicitly [11].

Let  $G$  be the  $m \times n$  matrix that has the property  $G\mathbf{u}_0 = \hat{\mathbf{u}}_0$ . For the diagonal Gaussian density we find

$$E[u_{0i} | \hat{\mathbf{u}}_0] = \sum_{k=1}^m q_{ik} u_{0k} + c_i \quad (4.4)$$

for  $i = 1, \dots, n$  where  $q_{ik}$  are the entries of the  $n \times m$  matrix  $Q$  and  $c_i$  are the entries of the  $n$ -vector  $\mathbf{c}$  given respectively by

$$Q = (CG^*)(GCG^*)^{-1} \quad (4.5)$$

$$\mathbf{c} = \mu - (CG^*)(GCG^*)^{-1}(G\mu), \quad (4.6)$$

where  $C$  is the covariance matrix of the Gaussian density with entries  $C_{jl} = E[(u_{0j} - \mu_j)(u_{0l} - \mu_l)^*] = A_{jl}$  and  $\mu$  is the vector of expectation values. Note that in the case of a diagonal Gaussian density, the entries  $q_{ik}$  for  $i = m+1, \dots, n$  and  $k = 1, \dots, m$  are zero. Hence, the conditional expectations of the unresolved modes conditioned on the resolved ones are equal to their unconditional expectations. This is as expected, because if the Gaussian is diagonal, the modes are independent from each other.

The conditional covariance matrix has entries

$$Cov[u_{0i}, u_{0j}^* | \hat{\mathbf{u}}_0] = E[u_{0i} u_{0j}^* | \hat{\mathbf{u}}_0] - E[u_{0i} | \hat{\mathbf{u}}_0] E[u_{0j}^* | \hat{\mathbf{u}}_0] = [C - QGC]_{ij}, \quad (4.7)$$

for  $i, j = 1, \dots, n$ . For the case of a diagonal Gaussian density, the entries of the conditional covariance matrix corresponding to interactions among resolved modes and their interaction with the unresolved modes are zero, for the same reasons explained above. Also, the entries of the covariance matrix for the interactions among unresolved modes are equal to the entries of the unconditional covariance matrix.

Wick's theorem holds for conditional expectations too [11]. Since we are dealing with complex variables, higher moments than the second consist of products of centered variables  $u_{0i} - E[u_{0i} | \hat{\mathbf{u}}_0]$  that have to be defined in a way that for even moments the resulting product is a positive number. For this reason we define the variable  $w_i = u_{0i}$  or  $w_i = u_{0i}^*$  depending on the product and find

$$E\left[\prod_{p=1}^P r_p | \hat{\mathbf{u}}_0\right] = \begin{cases} 0 & P \text{ odd,} \\ \sum_{perm} Cov[w_{i_1}, w_{i_2}^*]_{\hat{\mathbf{u}}_0} \dots Cov[w_{i_1}, w_{i_2}^*]_{\hat{\mathbf{u}}_0} & P \text{ even,} \end{cases} \quad (4.8)$$

where the summation is over all the possible pairings of the P indices and  $r_p = w_p - E[w_p|\hat{\mathbf{u}}_0]$ .

The nonlinear sum in (4.1) can be decomposed into 3 parts as

$$\sum_{\langle 1, \langle 2} u_{\langle 1} u_{\langle 2} + \sum_{\langle 1, \rangle 2} u_{\langle 1} u_{\rangle 2} + \sum_{\rangle 1, \rangle 2} u_{\rangle 1} u_{\rangle 2}, \quad (4.9)$$

where  $\sum_{\langle 1, \langle 2}$  indicates that we sum over all pairs of indices where both indices belong in the resolved range  $i = 1, \dots, m$ ,  $\sum_{\langle 1, \rangle 2}$  indicates summation over all pairs of indices where only one index is in the resolved range and  $\sum_{\rangle 1, \rangle 2}$  indicates summation over the pairs where both indices are outside the resolved range.

Using the decomposition above can facilitate the computation of the conditional expectations. We have

$$\begin{aligned} E[R_j(\mathbf{u}_0)|\hat{\mathbf{u}}_0] &= -\frac{ij}{2} \sum_{\langle 1, \langle 2} u_{0\langle 1} u_{0\langle 2} - \frac{ij}{2} \sum_{\langle 1, \rangle 2} u_{0\langle 1} E[u_{0\rangle 2}|\hat{\mathbf{u}}_0] \\ &\quad - \frac{ij}{2} \sum_{\rangle 1, \rangle 2} E[u_{0\rangle 1} u_{0\rangle 2}|\hat{\mathbf{u}}_0] + (j^2 - \nu j^4) u_{0j} \end{aligned} \quad (4.10)$$

For the quantity  $E[u_{0\rangle 2}|\hat{\mathbf{u}}_0]$  we have

$$E[u_{0\rangle 2}|\hat{\mathbf{u}}_0] = \sum_{l=1}^m q_{\rangle 2, l} u_{0l} + c_{\rangle 2}, \quad (4.11)$$

while for the quantity  $E[u_{0\rangle 1} u_{0\rangle 2}|\hat{\mathbf{u}}_0]$  we have

$$\begin{aligned} E[u_{0\rangle 1} u_{0\rangle 2}|\hat{\mathbf{u}}_0] &= E[u_{0\rangle 1} u_{0-\rangle 2}^*|\hat{\mathbf{u}}_0] \\ &= [C - QGC]_{0\rangle 1, 0-\rangle 2} + E[u_{0\rangle 1}|\hat{\mathbf{u}}_0] E[u_{0-\rangle 2}^*|\hat{\mathbf{u}}_0]. \end{aligned} \quad (4.12)$$

The expressions (4.10), (4.11) and (4.12) determine the Markovian term. If we use a diagonal Gaussian density, some of the terms in these expressions become zero. However, we kept the most general form for reasons of completeness of the presentation.

**4.2. Noise term.** The second term in (4.2) is the noise term  $QLu_{0j}$ , and we proceed with its calculation. From (4.3), (4.9) and (4.10) we have

$$\begin{aligned} QLu_{0j} &= -\frac{ij}{2} \sum_{\langle 1, \rangle 2} u_{0\langle 1} (u_{0\rangle 2} - E[u_{0\rangle 2}|\hat{\mathbf{u}}_0]) \\ &\quad - \frac{ij}{2} \sum_{\rangle 1, \rangle 2} (u_{0\rangle 1} u_{0\rangle 2} - E[u_{0\rangle 1} u_{0\rangle 2}|\hat{\mathbf{u}}_0]) \\ &= A_j(\mathbf{u}_0) + B_j(\mathbf{u}_0), \end{aligned} \quad (4.13)$$

where

$$A_j(\mathbf{u}_0) = -\frac{ij}{2} \sum_{\langle 1, \rangle 2} u_{0\langle 1} (u_{0\rangle 2} - E[u_{0\rangle 2}|\hat{\mathbf{u}}_0])$$

and

$$B_j(\mathbf{u}_0) = -\frac{ij}{2} \sum_{\rangle 1, \rangle 2} (u_{0\rangle 1} u_{0\rangle 2} - E[u_{0\rangle 1} u_{0\rangle 2}|\hat{\mathbf{u}}_0]).$$

Defining similarly  $A_j(\mathbf{u}(\mathbf{u}_0, s))$  and  $B_j(\mathbf{u}(\mathbf{u}_0, s))$  such that

$$e^{sL}QLu_{0j} = A_j(\mathbf{u}(\mathbf{u}_0, s)) + B_j(\mathbf{u}(\mathbf{u}_0, s))$$

we have in the short-memory approximation

$$\begin{aligned} \frac{\partial}{\partial t} e^{tL}u_{0j} &= e^{tL}\mathfrak{R}_j(\hat{\mathbf{u}}_0) \\ &+ A_j(\mathbf{u}(\mathbf{u}_0, t)) + \int_0^t e^{(t-s)L}PLQA_j(\mathbf{u}(\mathbf{u}_0, s))ds \\ &+ B_j(\mathbf{u}(\mathbf{u}_0, t)) + \int_0^t e^{(t-s)L}PLQB_j(\mathbf{u}(\mathbf{u}_0, s))ds \end{aligned} \quad (4.14)$$

From (4.13) and (4.14) we see that each one of the sums  $\sum_{<1, >2}$  and  $\sum_{>1, >2}$  make a contribution to the memory and the noise. We should mention here that the emergence and significance of multiplicative noise terms like the one coming from the sum  $\sum_{<1, >2}$  have been also discussed in the context of the stochastic modelling reduction strategy of Majda *et al.* [25, 26].

For the choices that we will make for the set of resolved variables, we can safely remove the contribution to the memory and the noise that comes from  $\sum_{>1, >2}$  as small due to the stiffness of the system; the stiffness of the KS system is due to the large ratio of growth rates between the small wavenumber modes and the large wavenumber modes that are present in the solution. In all the numerical experiments, the set of resolved variables includes mostly small wavenumber modes, thus the bulk of the unresolved modes are large wavenumber modes. These large wavenumber modes have small magnitude and thus the contribution of their interaction to the memory and noise through the term  $\sum_{>1, >2}$  is also small and thus can be neglected. However, recall that we retain the contribution of  $\sum_{>1, >2}$  to the Markovian (first) term  $\mathfrak{R}_j(\hat{\mathbf{u}}_0)$ .

The expression for  $A_j(\mathbf{u}(\mathbf{u}_0, t))$  involves quantities that are unknown, namely the modes  $u_{>2}(t)$ . We will approximate these modes as stochastic processes with known mean and autocorrelation by using the moving average method [15, 27, 39, 5]. Due to the fact that we are using a density that is non-invariant, the evolution of all the Fourier modes, and of the unresolved in particular, does not constitute a stationary stochastic process. However, for our numerical experiments we will treat the unresolved modes' evolution as a stationary stochastic process and use their statistics with respect to the initial density for the moving average method simulations. We defer the application of more sophisticated sample path generating methods suitable for nonstationary processes for future work.

Let  $u(t, \omega)$  be a wide sense stationary stochastic process. If its covariance

$$R(t_1, t_2) = E[(u(t_2, \omega) - m(t_2))(u(t_1, \omega) - m(t_1))^*]$$

is written as  $R(t_1, t_2) = \int e^{ik(t_2-t_1)}dF(k)$  for some non-decreasing function  $F(k)$  (through Khinchin's theorem) and also  $F(k)$  is such that  $dF(k) = \phi(k)dk$ , then

$$u(t, \omega) = \int h^*(s-t)\rho(ds) \quad (4.15)$$

where the function  $h(t)$  is the inverse Fourier transform of  $\hat{h}(k) = \sqrt{\phi(k)}$  and also,  $E[|\rho(ds)|^2] = ds$ . Note that the random measure  $\rho$  constructed as increments of Brownian motion at instants  $ds$  apart has this property. Thus, any wide-sense stationary

stochastic process with  $dF(k) = \phi(k)dk$  can be approximated as a sum of translates (in time) of a fixed function, each translate multiplied by independent Gaussian random variables. This is the "moving average" representation.

Having developed the formalism for the moving average representation, we now derive formulas for its numerical implementation. A possible approach would be to discretize the expression (4.15) in intervals of length  $\Delta t$  and use a midpoint rule to find

$$u(t_j) = \sum_{i=-n+j}^{n+j} h^*(t_i - t_j)\rho_i \quad (4.16)$$

with  $E[|\rho_i|^2] = \Delta t$  and  $t_j = j\Delta t$ . (4.16) can be rewritten (by the change of variables  $i' = i - j$  and dropping the primes) as

$$u(t_j) = \sum_{i=-n}^n h^*(t_i)\rho_{i+j} \quad (4.17)$$

and in effect the velocity at  $t_j$  is the dot product of a vector of values of  $h$  and a random vector. Recalling the remark above about the increments of Brownian motion, we see that the process  $u$  can be represented as a sum of suitably weighted Gaussian independent random variables with mean zero and variance  $\Delta t$ . In the numerical experiments, we split each unresolved mode in its real and imaginary parts which are approximated independently.

**4.3. Memory term.** After computing the Markovian and noise terms, we proceed with the calculation of the memory term

$$\int_0^t e^{(t-s)L} PLQA_j(\mathbf{u}(\mathbf{u}_0, s))ds. \quad (4.18)$$

Note that as in the case of the noise we only use the part of the memory that comes from the  $\sum_{<1, >2}$  terms in the convolution sums. We will use two different projections  $P$ , namely the linear and the finite-rank one. The conditional expectation projection will not be used because lack of explicit expressions make it computationally very expensive.

**4.3.1. Linear projection.** For a function  $g(\mathbf{u}_0)$  the linear projection is

$$(Pg)(\hat{\mathbf{u}}_0) = \sum_{i,j=1}^m b_{ij}^{-1}(g, u_{0i})u_{0j} \quad (4.19)$$

where  $b_{ij}^{-1}$  are the entries of a matrix whose inverse has entries  $b_{ij} = (u_{0i}, u_{0j})^*$  and the inner product is defined through the density  $f(x)$  (Gaussian in our case) as

$$(g, h) = \int_{-\infty}^{+\infty} g(x)h^*(x)f(x)dx dx^*.$$

Using (4.19) we have

$$\begin{aligned} \int_0^t e^{(t-s)L} PLQA_j(\mathbf{u}(\mathbf{u}_0, s))ds = & \quad (4.20) \\ \int_0^t e^{(t-s)L} \sum_{i,k=1}^m b_{ik}^{-1}(LQA_j(\mathbf{u}(\mathbf{u}_0, s)), u_{0i})u_{0k}ds. & \end{aligned}$$

What remains to be done is to compute the quantity  $LQA_j(\mathbf{u}(\mathbf{u}_0, s))$ . Some algebra and use of the relation

$$\sum_{l=1}^n R_l(\mathbf{u}_0) \frac{\partial}{\partial u_{0l}} A_j(\mathbf{u}(\mathbf{u}_0, s)) = \sum_{l=1}^n R_l(\mathbf{u}(\mathbf{u}_0, s)) \left( \frac{\partial A_j}{\partial u_{0l}} \right) (\mathbf{u}(\mathbf{u}_0, s)),$$

gives

$$\begin{aligned} LQA_j(\mathbf{u}(\mathbf{u}_0, s)) = & \quad (4.21) \\ & \sum_{l=1}^n R_l(\mathbf{u}(\mathbf{u}_0, s)) \left( \frac{\partial A_j}{\partial u_{0l}} \right) (\mathbf{u}(\mathbf{u}_0, s)) - \sum_{i,k=1}^m b_{ik}^{-1} (A_j(\mathbf{u}(\mathbf{u}_0, s)), u_{0i}) R_k(\mathbf{u}_0). \end{aligned}$$

Then the quantities  $(LQA_j(\mathbf{u}(\mathbf{u}_0, s)), u_{0i})$  can be computed by sampling the density via Monte Carlo, evolving the full system and averaging.

**4.3.2. Finite-rank projection.** The finite-rank projection of a function  $g(\mathbf{u}_0)$  on a finite number of terms of an orthonormal set of functions  $h_1(\hat{\mathbf{u}}_0), h_2(\hat{\mathbf{u}}_0), \dots$  is

$$(Pg)(\hat{\mathbf{u}}_0) = \sum_{i=1}^l (g, h_i) h_i, \quad (4.22)$$

where the inner product is defined as before and  $(h_i, h_j) = \delta_{ij}$ . Due to the fact that we are using a complex Gaussian density we can define an orthonormal set of functions by suitably modifying one-dimensional Hermite polynomials for each of the  $m$  resolved variables. Let  $\hat{\mathbf{u}}_0 = (u_{01}, \dots, u_{0m})$  be the vector of initial values of the resolved variables, where  $u_{0j} = z_{j1} + iz_{j2}$ . Define the  $2m$ -dimensional real vectors

$$\mathbf{z} = (z_{11}, z_{12}, \dots, z_{m1}, z_{m2})$$

and

$$\boldsymbol{\mu} = (\mu_{11}, \mu_{12}, \dots, \mu_{m1}, \mu_{m2}).$$

We need to split each mode in its real and imaginary parts because of the definition of the orthonormal set below.

We define the multi-index  $\boldsymbol{\kappa} = (\kappa_1, \dots, \kappa_m)$  and the set of functions

$$h^\boldsymbol{\kappa}(\mathbf{z}) = \prod_{j=1}^m [\tilde{H}_{\kappa_j}(\sqrt{\frac{2}{a_j}}(z_{j1} - \mu_{j1})) + i\tilde{H}_{\kappa_j}(\sqrt{\frac{2}{a_j}}(z_{j2} - \mu_{j2}))], \quad (4.23)$$

where

$$\tilde{H}_{\kappa_j}(x) = \frac{1}{\sqrt{2}} (1 + 2\beta_{\kappa_j})^{\frac{1}{4}} H_{\kappa_j}((1 + 2\beta_{\kappa_j})^{\frac{1}{2}} x) e^{-\frac{\beta_{\kappa_j}}{2} x^2}. \quad (4.24)$$

The functions  $H_{\kappa_j}$  are Hermite polynomials (with weight  $\exp(-\frac{1}{2}x^2)$ ) satisfying

$$H_0(x) = 1, \quad H_1(x) = x, \quad H_k(x) = \frac{1}{\sqrt{k}} x H_{k-1}(x) - \sqrt{\frac{k-1}{k}} H_{k-2}(x) \quad (4.25)$$

and  $\beta_{\kappa_j} > -\frac{1}{2}$ . The derivatives of the functions  $\tilde{H}_{\kappa_j}(x)$  can be computed by the recursive relation

$$\frac{d}{dx} \tilde{H}_{\kappa_j}(x) = (1 + 2\beta_{\kappa_j})^{\frac{1}{2}} \tilde{H}_{\kappa_j-1}(x) - \beta_{\kappa_j} x \tilde{H}_{\kappa_j}(x). \quad (4.26)$$



To ensure the orthonormality of the above set of functions, we have to impose a constraint on the values of the entries of the multi-index  $\kappa$ . The constraint is, that the entries corresponding to a positive wavenumber and its corresponding negative wavenumber cannot be simultaneously different from zero. We, also, have to enforce the constraint  $\beta_{\kappa_j} = 0$  when  $H_{\kappa_j}$  is of order zero. These constraints arise from the fact that the solution of Kuramoto-Sivashinsky equation is real thus the  $k$ -th negative Fourier mode is the complex conjugate of the  $k$ -th positive mode.

The memory term becomes

$$\int_0^t e^{(t-s)L} PLQA_j(\mathbf{u}(\mathbf{u}_0, s)) ds = \int_0^t e^{(t-s)L} \sum_{\kappa \in I} (LQA_j(\mathbf{u}(\mathbf{u}_0, s)), h^\kappa(\hat{\mathbf{u}}_0)) h^\kappa(\hat{\mathbf{u}}_0) ds,$$

where

$$\begin{aligned} LQA_j(\mathbf{u}(\mathbf{u}_0, s)) = & \sum_{i=1}^n R_i(\mathbf{u}(\mathbf{u}_0, s)) \left( \frac{\partial A_j}{\partial u_{0i}} \right) (\mathbf{u}(\mathbf{u}_0, s)) \\ & - \sum_{i=1}^m R_i(\mathbf{u}_0) \sum_{\kappa \in I} (A_j(\mathbf{u}(\mathbf{u}_0, s)), h^\kappa(\hat{\mathbf{u}}_0)) \frac{\partial h^\kappa(\hat{\mathbf{u}}_0)}{\partial u_{0i}} \end{aligned}$$

and  $I$  denotes the set of  $m$ -tuples of indices used in the finite-rank projection.

Thus, we see that starting from the short-memory approximation we have transformed the original system of ODEs into a system of random ordinary integrodifferential equations. Such an approach was adopted in [1] and termed stochastic optimal prediction. In [1], the form of the projection coefficients allowed the reduction of the integrodifferential equations to differential equations (this is the delta-function approximation discussed earlier).

**5. Numerical simulations.** We use the short-memory approximation equations for the KS system to compute the evolution of the conditional expectations of a set of resolved Fourier modes conditioned on their initial values. We conducted numerical experiments for two sets of resolved variables. The first set includes all the modes that are linearly unstable (for the value of the viscosity used). The second set includes all but one linearly unstable modes. The error exhibited by the short-memory approximation is strikingly different for these two sets of resolved variables and we offer an explanation for this difference.

**5.1. Resolution of all unstable modes.** We present the results of the short-memory approximation for the first set of resolved variables that includes all the unstable modes.

**5.1.1. Linear projection.** In order to construct the short-memory approximation equations we have to compute the first (Markovian), second (noise) and third (memory) terms in the RHS of the short-memory approximation equation. The Markovian term can be computed explicitly, while the noise and memory terms rely on expressions that have to be computed through simulations of the full system.

For the value of viscosity  $\nu = 0.085$  used in our experiments, a truncation retaining the first  $N = 24$  modes is enough to fully resolve the system. Since two of the modes

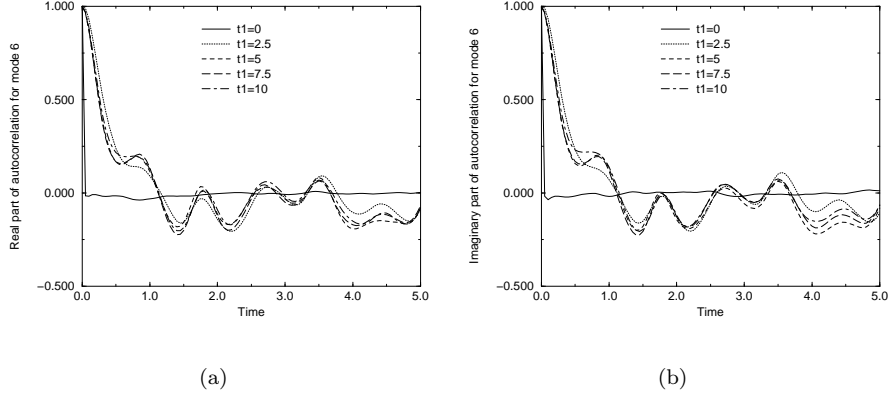


FIG. 5.1. Autocorrelation for the unresolved mode with wavenumber 6 for different initial times. a) Real part, b) Imaginary part.

are set to zero, the effective number of modes is  $n = N - 2 = 22$ . The  $n$ -dimensional system is called the full system. We assume that initially we know the values of only  $m$  of the  $n$  modes, while the values of the rest  $n - m$  modes are drawn from the diagonal Gaussian density (3.2). The  $m$  resolved modes constitute the reduced system. We examine the case where we know initially only  $\frac{N}{2} = 12$  variables. However, for the same reasons as in the case of the full system, the zeroth and -6th mode are set to zero, and the effective number of modes for the reduced system is  $12 - 2 = 10$ . We set  $m = 10$  in all subsequent calculations.

For the first set of resolved modes, the reduced system includes all the modes that are linearly unstable. For our case there are three positive and three negative wavenumber modes that are linearly unstable, namely the modes for  $k = -3, -2, -1, 1, 2, 3$ . The rest  $10 - 6 = 4$  modes in the resolved set are linearly stable modes, namely the modes with  $k = -5, -4, 4, 5$ .

We proceed with the presentation of the calculations for the quantities needed for the evaluation of the noise term  $A_j(\mathbf{u}(\mathbf{u}_0, t))$ . The noise term involves the unknown quantities  $u_{>2}(t)$ . Because we are using a density that is not invariant, the quantities  $u_{>2}(t)$  are nonstationary stochastic processes. Fig.(5.1) shows the autocorrelation for the unresolved mode with wavenumber 6

$$E[(u_6(t_2) - E[u_6(t_2)])(u_6(t_1) - E[u_6(t_1)])^*]$$

for different initial times  $t_1$ . As explained before, we approximate the quantities  $u_{>2}(t)$  as stationary stochastic processes with mean and autocorrelation determined with respect to the diagonal Gaussian density. We use the moving average method to sample these stochastic processes. Each of the unknown Fourier modes is split into its real and imaginary parts which are approximated independently. Fig.(5.2) shows the autocorrelation of the real and imaginary parts for the unresolved mode with wavenumber 6 as computed by the full system and the moving average method. The moving average method estimates for the autocorrelations of the unresolved modes were produced by averaging over 10000 sample paths.

After the properties of the noise term, we have to calculate the properties of the memory term. The quantities needed for the memory term evaluation were computed

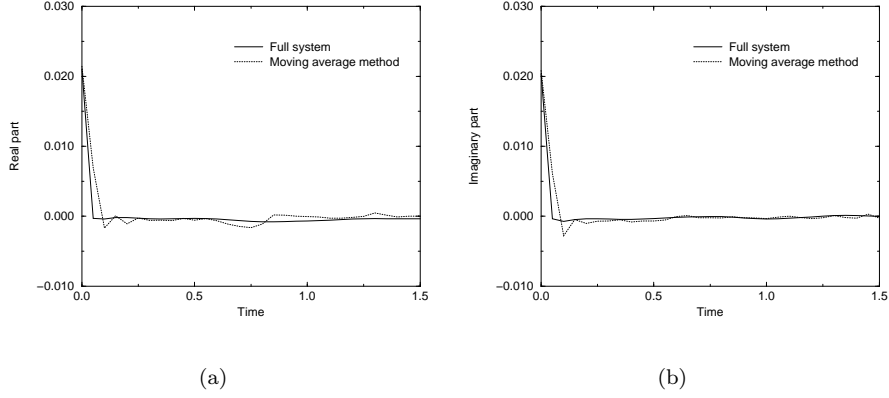


FIG. 5.2. Comparison of the autocorrelation for the unresolved mode with wavenumber 6 as computed from the full system and the moving average method. a) Real part, b) Imaginary part.

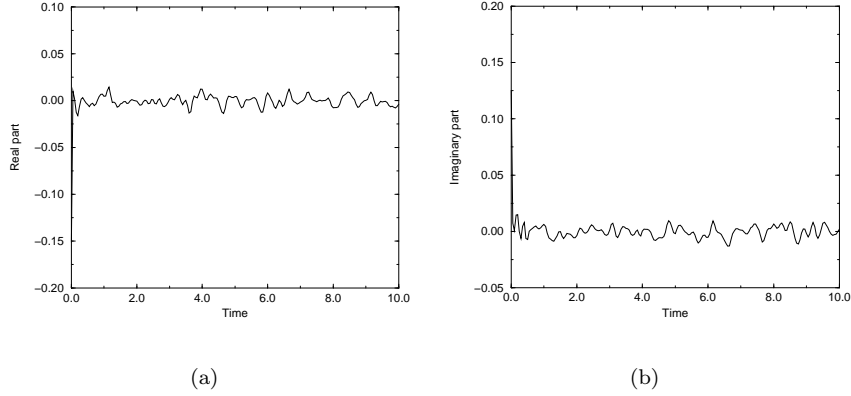


FIG. 5.3. Projection coefficient of the memory term for the equation for the resolved mode 1 on the resolved mode 4 for the first set of variables. a) Real part, b) Imaginary part.

averaging over 10000 samples. For the case of the linear projection, we have to compute the term (recall (4.20))

$$\int_0^t e^{(t-s)L} \sum_{i,k=1}^m b_{ik}^{-1}(LQA_j(\mathbf{u}(\mathbf{u}_0, s)), u_{0i})u_{0k}ds,$$

so we need to compute the projection coefficients  $\sum_{i,k=1}^m b_{ik}^{-1}(LQA_j(\mathbf{u}(\mathbf{u}_0, s)), u_{0i})$ . Fig.(5.3) shows the evolution of the projection coefficient of the memory term for the equation for the resolved mode with wavenumber 1 on the resolved mode 4  $\sum_i b_{i4}^{-1}(LQA_1(\mathbf{u}(\mathbf{u}_0, s)), u_{0i})$  (from now on we omit the word wavenumber for aesthetic reasons).

Inspection of the behavior of all the projection coefficients needed in the memory term determination reveals that the coefficients decay fast in time. The fast decay of the quantities  $(LQe^{sL}QLu_j, u_k)$ , i.e. of the projection coefficients in the short-memory approximation, can only guarantee the fast decay of the quantities  $(LQe^{sQL}QLu_j, u_k)$

of the exact Mori-Zwanzig equation for short times. For large times, the quantities  $(LQe^{sQL}QLu_j, u_k)$  can behave very differently from  $(LQe^{sL}QLu_j, u_k)$ . Thus, we have to truncate the interval of integration for the integral term from  $[0, t]$  to  $[t - t_0, t]$  (for  $t > t_0$ ). The time  $t_0$  is a short time over which the error of using  $(LQe^{sL}QLu_j, u_k)$  instead of  $(LQe^{sQL}QLu_j, u_k)$  is not large. Of course, we do not know the value of  $t_0$  beforehand, since we do not know the quantities  $(LQe^{sQL}QLu_j, u_k)$ . However, motivated by the numerically determined form of the projection coefficients  $(LQe^{sL}QLu_j, u_k)$ , we truncate the interval of integration for the memory term from  $[0, t]$  to  $[t - 1, t]$  (for  $t > 1$ ), since most projection coefficients decay significantly in a time interval of length 1.

The determination of the properties of the noise and the memory allows us to solve the short-memory approximation equations for the resolved modes. Although the full system is stiff, since it includes many stable modes with very large decay rates, the stable modes contained in the reduced system have small decay rates. This allows us to use an explicit solver for the reduced system. For our numerical experiments we use the Runge-Kutta 4th order method to solve the random integrodifferential equations of the short-memory approximation. For the calculation of the integral memory term we used two different methods, namely the trapezoidal rule and Simpson's rule. Most experiments were done twice, once with each method.

The quantities used in the noise term have very fast decaying autocorrelations, which result in a rough (in time) noise. This, in turn, can create problems with the numerical stability of the explicit solver. However, the noise has small magnitude and does not appear to create problems in the actual implementation.

The system of random integrodifferential equations is solved over and over for different realizations of the noise. The initial condition used for the resolved modes with wavenumbers  $-3, -2, -1, 1, 2, 3$  is  $u_1 = u_{-1} = u_2 = u_{-2} = u_3 = u_{-3} = 1$ , while the rest of the resolved modes are set initially equal to zero. The conditional expectations of the resolved modes conditioned on their initial values are computed by averaging over the realizations of the noise.

The truth is computed as follows. We sample the density over and over keeping the resolved modes fixed to the values just described. For each sample, we evolve (3.1) for  $k = -11, \dots, 11$ . Finally, we average over the samples and obtain the conditional expectations of the resolved modes.

The Galerkin approximation consists of setting the unresolved modes equal to zero for all times, i.e. solving (3.1) for  $k = -5, \dots, 5$ . For the Galerkin approximation there is no need to solve the reduced system repeatedly, because for each realization the unresolved modes are set equal to zero.

Figs.(5.4), (5.5), (5.6) show the real and imaginary parts of the short-memory approximation estimates of the conditional expectations for the resolved modes 1,2,3 as compared to the truth and the Galerkin approximation. The true conditional expectations were computed by averaging over 1000 samples. The short-memory estimates were computed by averaging over 1000 realizations of the noise. The results for the truth and the optimal prediction estimates are converged, even with a 1000 samples, because, the unresolved modes have small magnitudes. However, there is no "slaving" [13] of the unresolved modes to the resolved ones. The randomness in the initial conditions of the unresolved modes does affect the conditional expectations of the resolved ones. However, in the time interval that we examine, the results of the randomness of the initial conditions have not yet fully manifested themselves, and thus 1000 samples (or 1000 realizations of the noise) are enough for convergence of

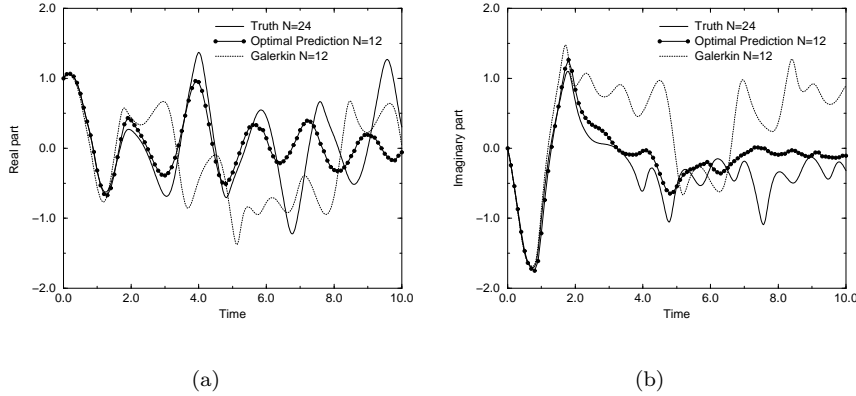


FIG. 5.4. Conditional expectation evolution for the resolved mode 1 for the first set of resolved variables. a) Real part, b) Imaginary part.

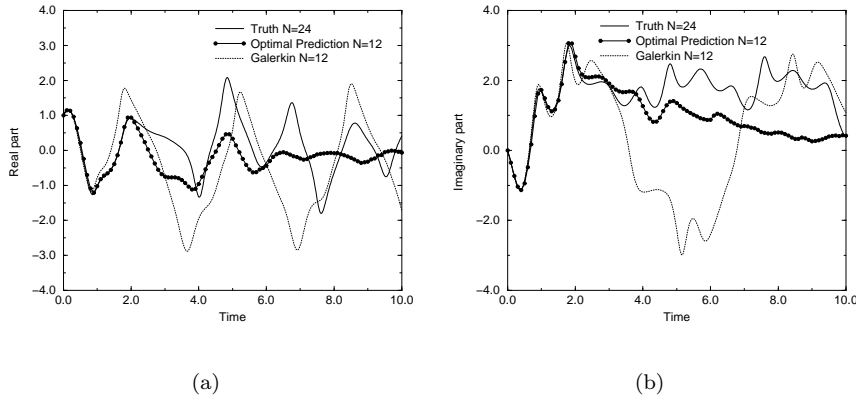


FIG. 5.5. Conditional expectation evolution for the resolved mode 2 for the first set of resolved variables. a) Real part, b) Imaginary part.

the results. For longer times, more samples (or realizations of the noise) are needed for convergence of the truth and the optimal prediction estimates.

As can be seen, there is good agreement between the short-memory approximation estimates for the conditional expectations of the resolved modes and the true conditional expectations of these modes. Also, the short-memory approximation results constitute a considerable improvement over the results for the Galerkin approximation. The good agreement of the short-memory estimates for the conditional expectations of the resolved modes, indicates that the fast decay of the projection coefficients ( $LQe^{sQL}QLu_j, u_k$ ) is not restricted to short times only. On the contrary, they must continue to decay fast for larger times and this allows the short-memory approximation to perform well.

Motivated by the fact that all the projection coefficients ( $LQe^{sL}QLu_j, u_k$ ) used in the short-memory approximation decay fast, we can inquire about the validity of an even more drastic approximation which replaces the projection coefficients by delta-

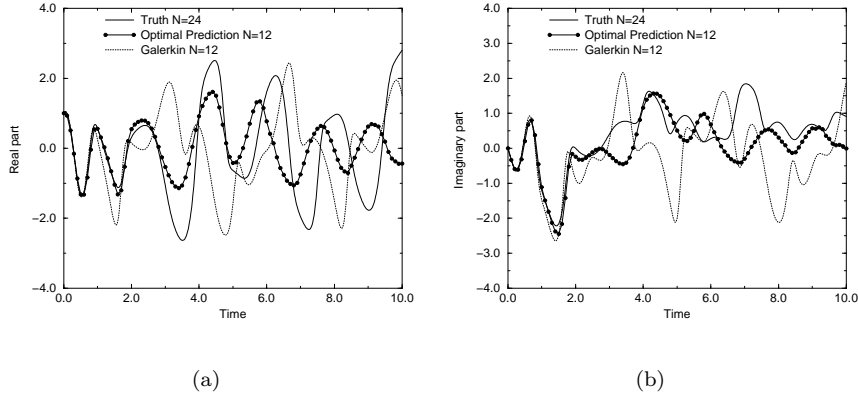


FIG. 5.6. *Conditional expectation evolution for the resolved mode 3 for the first set of resolved variables. a) Real part, b) Imaginary part.*

functions multiplied by the integrals of the quantities  $(LQe^{sL}QLu_j, u_k)$ . Of course, as before, these integrals must be computed over a truncated interval. The advantage of such an approximation is that the reduced system is a system of random ordinary differential equations and not integrodifferential equations. This results in a significant reduction of the computational time needed to calculate the estimates of the conditional expectations of the resolved modes. Fig.(5.7) show the estimate of the conditional expectation for the resolved mode 1 using the delta-function approximation, compared to the results of the short-memory approximation and the truth. The delta-function approximation can predict accurately the evolution of the conditional expectation for shorter times than the short-memory approximation. The inadequacy of the delta-function approximation to predict the evolution of the conditional expectations for longer times can be explained by a more careful inspection of the projection coefficients  $(LQe^{sL}QLu_j, u_k)$ . Although these coefficients decay fast, several of them do not retain the same sign during this decay (see e.g. Fig.(5.8)). In fact, they oscillate rapidly with non-negligible amplitudes. Integration of these oscillations results in cancellations that lead to loss of important information about the short-time memory. As a result, the delta-function approximation loses accuracy. However, the accuracy exhibited by the delta-function approximation is impressive, if we consider that it results in a system of differential (and not integrodifferential) differential equations whose numerical integration is very fast. For our numerical experiments, the integration of the delta-function approximation equations is 15 times faster than the integration of the short-memory approximation equations. In fact, the time of integration, for one realization of the noise, of the delta-function approximation equations, is comparable to the time of integration of the equations for the simple Galerkin approximation.

**5.1.2. Finite-rank projection.** We conclude our presentation of results for the first set of variables with the estimates of the conditional expectations obtained when we use the finite-rank projection in the memory term calculations.

Fig.(5.9) shows the real and imaginary parts of the finite-rank projection short-memory approximation estimates of the conditional expectations for the resolved mode 1, as compared to the truth and the linear projection short-memory approxi-

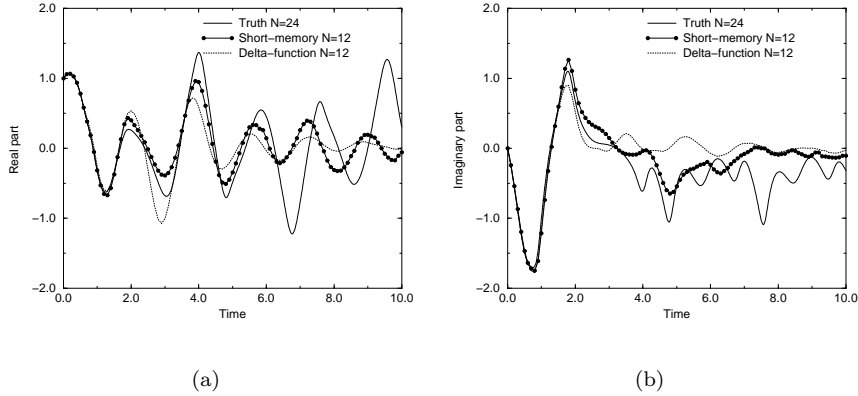


FIG. 5.7. *Conditional expectation evolution for the resolved mode 1 for the first set of resolved variables. Delta-function vs short-memory. a) Real part, b) Imaginary part.*

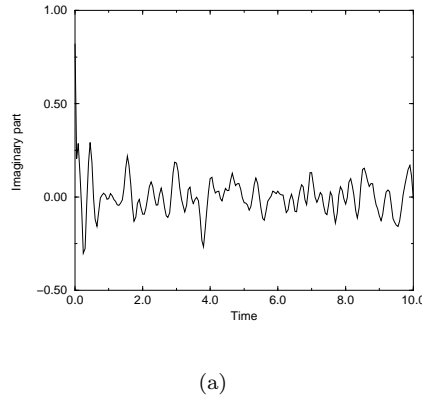


FIG. 5.8. *Imaginary part of the projection coefficient of the memory term for the equation for the resolved mode 5 on the resolved mode 1 for the first set of resolved variables.*

mation estimates. The finite-rank projection short-memory approximation estimates were computed by averaging over 1000 realizations of the noise. For our numerical experiments we use the value  $\beta_{\kappa_j} = 0$  for all  $H_{\kappa_j}$ , irrespective of their order (see 4.23-4.25). Note that when  $\beta_{\kappa_j} = 0$ , the first order polynomials in the set are the functions used in the linear projection (with a different numerical factor coming from the orthonormality of the set functions). The finite-rank projection estimates are computed using polynomials of order up to 2 for the two most unstable modes. All the constraints mentioned above result in a set of 30 orthonormal functions (we also omit the function that consists of polynomials of order zero in each mode, which is a constant). The interval of integration of the memory term was truncated from  $[0, t]$  to  $[t - 1, t]$ . Different truncations did not alter the results much.

The finite-rank projection estimates of the conditional expectations are worse than the linear projection ones. This result, although surprising at first, can be explained by examining the assumption under which the short-memory approximation

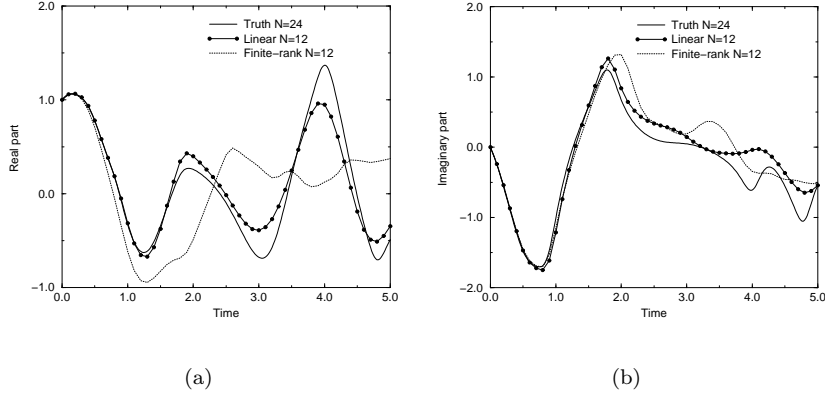


FIG. 5.9. *Conditional expectation evolution for the resolved mode 1 for the first set of resolved variables. Linear vs. finite-rank projection for the memory. a) Real part, b) Imaginary part.*

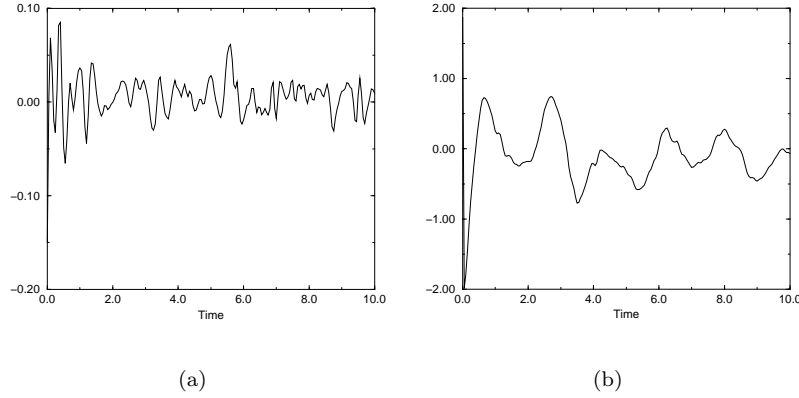


FIG. 5.10. *Examples of slowly-decaying projection coefficients of the memory term on polynomials of order higher than 1. Finite-rank projection for the first set of resolved variables.*

is expected to be valid for long times. The short-memory approximation is valid if the quantities  $(LQe^{sQL}QLu_j, h_k)$  decay fast and stay small for long times. If they do not, then the short-memory approximation is valid for short times only. Also, the behavior of the quantities  $(LQe^{sL}QLu_j, h_k)$  can only be used to infer the behavior of  $(LQe^{sQL}QLu_j, h_k)$  for short times. Inspection of the projection coefficients  $(LQe^{sL}QLu_j, h_k)$  for the case of the finite-rank projection reveals that several of these coefficients, do not decay fast. This means that, at least for short times, the quantities  $(LQe^{sQL}QLu_j, h_k)$  do not decay fast. Since the conditional expectation estimates based on the finite-rank projection are not good for longer times, we conclude that the quantities  $(LQe^{sQL}QLu_j, h_k)$  do not start decaying fast after a short time. This is not contradictory with the notion that the finite-rank projection is a more accurate projection than the linear one. Indeed, the finite rank projection is better than the linear one for the memory term of the exact Mori-Zwanzig equation and for the memory term of the short-memory approximation. However, being a more accurate



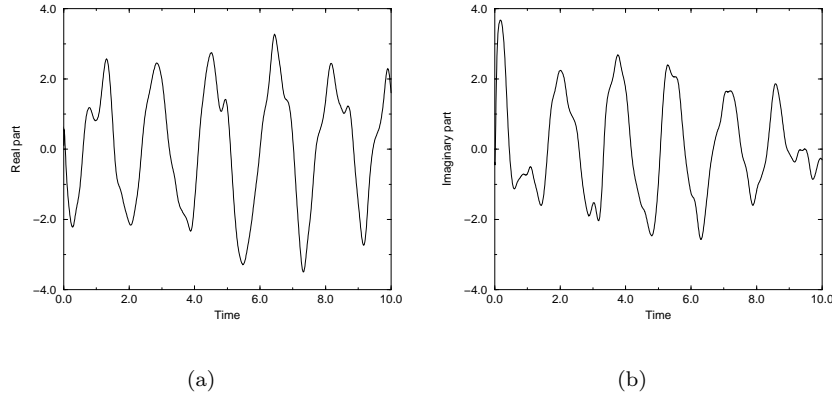


FIG. 5.11. *Projection coefficient of the memory term for the equation for the resolved mode 2 on the resolved mode 4 for the second set of resolved variables. a) Real part, b) Imaginary part.*

projection, does not necessarily guarantee that the projection coefficients on polynomials of order higher than 1 (recall  $\beta_{\kappa_j} = 0$ ) have to decay fast and stay small for long times. This is exactly what happens in our case. Several projection coefficients ( $LQe^{sQL}QLu_j, h_k$ ) on polynomials of order higher than 1 do not decay fast and do not stay small for long times, thus violating the short-memory approximation assumption. In this way, the short-memory approximation for the linear projection case that does not include those slowly-decaying coefficients, is better than the short-memory approximation for the finite-rank projection that does include those slowly-decaying projection coefficients. Fig.(5.10) shows some examples of slowly decaying projection coefficients on polynomials of order larger than 1.

**5.2. Resolution of all but one unstable modes.** For the second set of resolved modes, we include in the resolved modes all the linearly unstable modes except for one. We choose to leave the modes  $k = -1, 1$  as unresolved. There is no particular reason for this choice. Any other unstable mode can be left as unresolved, since it is the instability, and not the growth rate, of an unresolved mode that determines the accuracy of the short-memory approximation. In fact, for our value of the viscosity, mode 1 has the smallest (linear) growth rate among the unstable modes. With this choice, the set of resolved modes contains the unstable modes  $k = -3, -2, 2, 3$  and the stable modes  $k = -6, -5, -4, 4, 5, 6$ . As in the case of the first set of resolved variables, the full system has  $n = 22$  modes and the reduced system  $m = 10$  modes. For the second set of resolved variables, we only conducted numerical experiments where the linear projection was used for the memory term.

Fig.(5.11) shows the typical behavior of the projection coefficients. As is evident, the projection coefficients ( $LQe^{sL}QLu_j, u_k$ ) of the short-memory approximation do not decay fast. There are still some coefficients that decay fast, but the majority of the projection coefficients do not and those determine the accuracy of the conditional expectation estimate. We only know (recall (2.7)) that the coefficients ( $LQe^{sL}QLu_j, u_k$ ) approximate well the quantities ( $LQe^{sQL}QLu_j, u_k$ ) for short times. Even though the coefficients ( $LQe^{sL}QLu_j, u_k$ ) of the short-memory approximation do not decay fast, the coefficients ( $LQe^{sQL}QLu_j, u_k$ ) can very well start decaying fast after a short time. However, we don't know that before implementing the short-time approximation. By

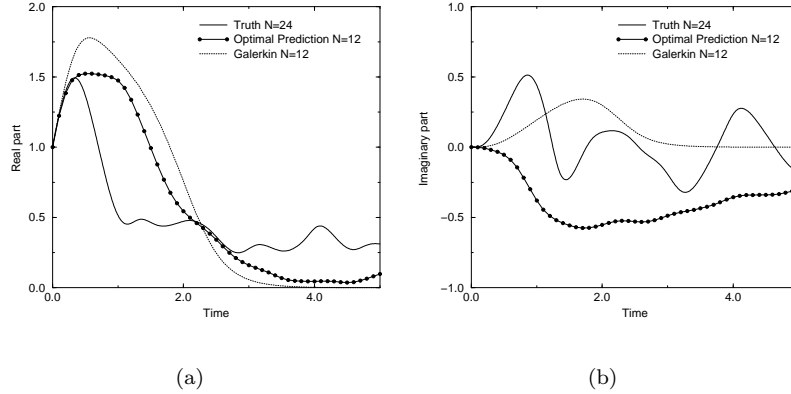


FIG. 5.12. *Conditional expectation evolution for the resolved mode 2 for the second set of resolved variables. a) Real part, b) Imaginary part.*

the same reasoning as in the case of resolution of all unstable modes, we have to truncate the interval of integration for the memory term, from  $[0, t]$  to  $[t - t_0, t]$  (for  $t > t_0$ ). Again,  $t_0$  is a short time over which the error of using  $(LQe^{sL}QLu_j, u_k)$  instead of  $(LQe^{sQL}QLu_j, u_k)$  is not large. Of course, we do not know the value of  $t_0$ . In the case of resolution of all unstable modes, we guessed that the interval  $t_0$  should be close to the time needed for the projection coefficients to decay significantly. But, in the present case, where the projection coefficients do not decay fast, we cannot make any guess. We conducted numerical experiments with different truncated intervals of integration for the memory term and the results do not change much. We present results for the case where the interval of integration of the memory term is truncated from  $[0, t]$  to  $[t - 1, t]$  (for  $t > 1$ ).

The system of random integrodifferential equations is solved repeatedly for different realizations of the noise. The initial condition for the resolved modes  $-3, -2, 2, 3$  is  $u_2 = u_{-2} = u_3 = u_{-3} = 1$ , while the rest of the resolved modes are set initially equal to zero.

Figs.(5.12), (5.13), (5.14) show the real and imaginary parts of the short- memory estimates of the conditional expectations for the resolved modes 2,3,4 as compared to the truth and the Galerkin approximation. The true conditional expectations were computed by averaging over 10000 samples. The short-memory estimates were computed by averaging over 10000 realizations of the noise. As can be seen, there is good agreement between the short-memory approximation estimates for the conditional expectations of the resolved modes and the true conditional expectations of these modes only for very short times. For longer times the errors become large.

We show next that the results for the short-memory approximation depend mostly on the accuracy with which we approximate the memory term, and not so much on the accuracy of the approximation of the noise term. It is instructive to integrate the optimal prediction equations in the short-memory approximation with the memory term set to zero. Fig.(5.15) shows the conditional expectation estimate for the resolved mode 2 as predicted by the short-memory approximation when the memory term is set to zero. We compare it to the truth and the short-memory approximation when the memory term is not set to zero. As is evident, the estimate is good for short

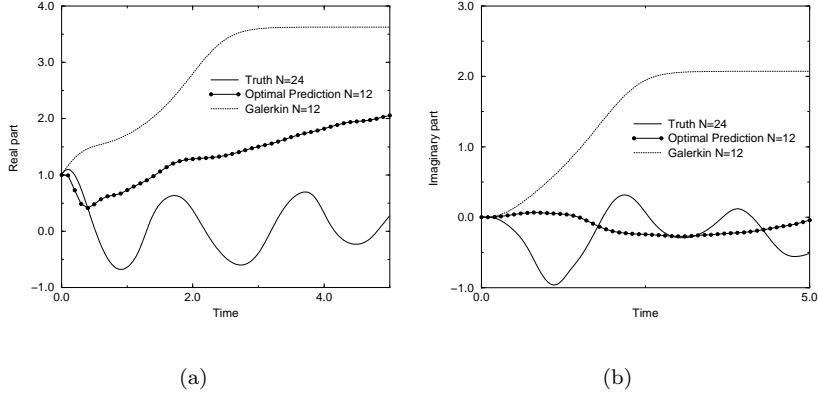


FIG. 5.13. *Conditional expectation evolution for the resolved mode 3 for the second set of resolved variables. a) Real part, b) Imaginary part.*

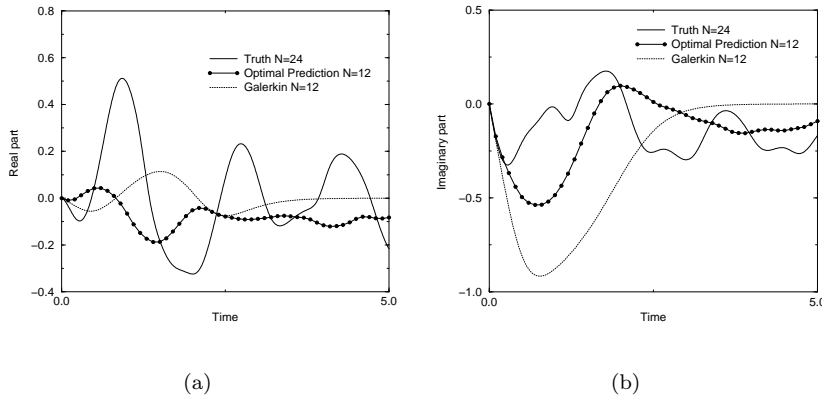


FIG. 5.14. *Conditional expectation evolution for the resolved mode 4 for the second set of resolved variables. a) Real part, b) Imaginary part.*

times, while for longer times, the estimate converges to zero. Any deviations of the conditional expectations from zero, i.e. any improvement of the estimate, must be produced by the memory term. The deviations from zero, for long times, of the true conditional expectations, translate into memory effects for the set of resolved modes, and if these memory effects are not well represented in the model for the resolved modes, the prediction of the deviations is not accurate.

Since the short-memory approximation estimates are not good for long times, we conclude that the quantities  $(LQe^{sQL}QLu_j, u_k)$  do not start decaying fast after a short time. If they did, the short-memory approximation would give good results for longer times. The inclusion of an unstable mode in the unresolved modes, results in the appearance of long-time memory effects, but the precise mechanism of formation of these long-time memory effects has yet to be determined.

For the second set of variables, no attempt was made to compute the conditional expectation estimates using the finite-rank projection or the delta-function approxi-

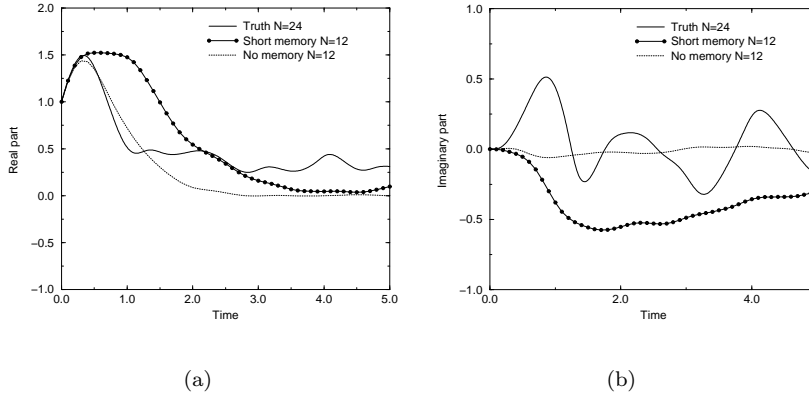


FIG. 5.15. Comparison of the conditional expectation evolution estimates for the resolved mode 2, as produced by the short-memory approximation and the short-memory approximation with the memory term set to zero. a) Real part, b) Imaginary part.

mation. For the case of the finite-rank projection, there is no chance of improvement, since the linear projection coefficients that are part of the finite-rank projection, are already slowly-decaying. For the case of the delta-function approximation, there is no incentive to try it, since the projection coefficients do not decay fast.

**6. Conclusions.** We have applied the optimal prediction formalism to the solutions of the Kuramoto-Sivashinsky equation in a Fourier-Galerkin truncation when some initial data are missing. The conditional expectations of the resolved modes conditioned on their initial values were estimated through simulation of the optimal prediction equations and compared to the true conditional expectations computed from simulations of the full system. The results of the comparison depend on which Fourier modes are contained in the set of resolved variables and on the type of projection used in the memory term. For the case when the resolved variables include all the unstable modes, we used two different kinds of projection for the memory term, namely the linear projection and the finite-rank one.

For the linear projection, the agreement between the optimal prediction estimates of the conditional expectations and the true conditional expectations is good for relatively long times. Also, the estimates show a considerable improvement over the Galerkin approximation, where we resolve a reduced set of variables and set all the unresolved variables equal to zero. For the case of the linear projection we, also, tried the more drastic delta-function approximation where the correlations appearing in the memory term integrand are replaced by a delta-function multiplied by the integral. In this case, the resulting optimal prediction equations are differential (not integrodifferential) equations. The results are not as good as in the more sophisticated short-memory approximation. However, the accuracy of the conditional expectation estimates based on the delta-function approximation is impressive, if we consider the much greater numerical efficiency of the resulting system of equations for the resolved modes.

For the finite-rank projection, the agreement is good only for short times. The growth of the error for larger times is due to the fact that the short-memory approximation assumption is violated by the appearance of long-time memory effects. These

manifest themselves as slowly-decaying projection coefficients in the memory term integral.

For the case where one unstable mode is left unresolved, we used only the linear projection. The error of the estimates of the conditional expectations becomes large after a short time. The growth of the error is due to the fact that the short-memory approximation assumption is violated by the appearance of long-time memory effects. The short-memory approximation estimates of the conditional expectations are still an improvement over the Galerkin approximation estimates. For the case where one unstable mode is left unresolved, we did not attempt to use the finite-rank projection, since the linear projection that is part of the finite-rank projection, already violates the short-memory approximation.

In the case of the finite-rank projection for the first set of resolved modes, the long-time memory effects are a result of projecting on polynomials of the resolved modes of order higher than 1. For the second set of resolved modes, where we used the linear projection for the memory term, the long-time memory effects are a result of leaving an unstable mode as unresolved. Although the long-time memory effects for these two cases have different causes, the result is the same, namely the violation of the short-memory approximation assumption. This leads to a large increase of the error in the conditional expectation estimates after a short time. The inadequacy of the short-memory approximation to produce accurate estimates of the conditional expectations for long times, suggests that for cases with slowly-decaying projection coefficients, the calculation of the quantities  $(LQe^{sQL}QLu_j, u_k)$  cannot be avoided (see [9] for methods of computing these quantities).

The determination of the reasons for the appearance of long-time memory effects is important since it can provide insight on the way that the partial information known initially is lost when we perform underresolved computations. It can also help in determining which variables (or combinations of variables) of the full system should be resolved, if we hope to obtain a reduced model of the system that is accurate for long times [7, 17].

**Acknowledgments.** The work presented here is part of my doctoral thesis [35], and was conducted under the supervision of Professor Alexandre Chorin of UC Berkeley while I was a guest at the Lawrence Berkeley National Laboratory. I would like to thank Professor Chia-Kun Chu of Columbia University in New York for his generous support. Also, I would like to thank Dr. Kevin Lin and Dr. Mayya Tokman of UC Berkeley for very helpful discussions and comments.

#### REFERENCES

- [1] J. BELL, A. CHORIN, AND W. CRUTCHFIELD, *Stochastic optimal prediction with applications to averaged Euler equations*, in Proceedings of the Seventh National Conference on Computational Fluid Mechanics, Pingtung, Taiwan, C. Lin, ed., 2000, pp. 1–13.
- [2] K. BINDER AND D. HEERMANN, *Monte Carlo Simulation in Statistical Physics, An Introduction*, Springer, 1997.
- [3] L. BREIMAN, *Bagging predictors*, Machine Learning, 24 (1996), pp. 123–140.
- [4] D. CAI, D. MCLAUGHLIN, AND J. SHATAH, *Spatiotemporal chaos and effective stochastic dynamics for a near integrable nonlinear system*, Phys. Lett. A, 253 (1999), pp. 280–286.
- [5] C. CAMERON, *A Comparative Analysis of Methods for Sampling Stationary Stochastic Processes*, PhD thesis, Department of Mathematics, University of California Berkeley, 2003.
- [6] C. CANUTO, M. HUSSAINI, A. QUARTERONI, AND T. ZANG, *Spectral Methods in Fluid Dynamics*, Springer-Verlag, 1988.
- [7] A. CHORIN, *Conditional Expectations and Renormalization*, Multiscale Modeling and Simulation, 1 (2003), pp. 105–118.

- [8] A. CHORIN, O. HALD, AND R. KUPFERMAN, *Optimal prediction and the Mori-Zwanzig representation of irreversible processes*, Proc. Natl. Acad. Sci. USA, 97 (2000), pp. 2968–2973.
- [9] ———, *Optimal prediction with memory*, Physica D, 166 (2002), pp. 239–257.
- [10] A. CHORIN, A. KAST, AND R. KUPFERMAN, *Optimal prediction of underresolved dynamics*, Proc. Natl. Acad. Sci. USA, 95 (1998), pp. 4094–4098.
- [11] ———, *On the prediction of large-scale dynamics using unresolved computations*, Contemporary Math., 238 (1999), pp. 53–75.
- [12] M. CROSS AND P. HOHENBERG, *Pattern formation outside of equilibrium*, Rev. Mod. Phys., 65 (1993), pp. 851–1112.
- [13] C. FOIAS, G. SELL, AND R. TEMAM, *Inertial manifolds for dissipative partial differential equations*, Proc. Acad. Sc. Paris, I (1985), pp. 285–288.
- [14] C. GEAR, *Numerical initial value problems in ordinary differential equations*, Prentice-Hall, 1971.
- [15] I. GIKHMAN AND A. SKOROKHOD, *The Theory of Stochastic Processes*, Springer, 1979.
- [16] E. HAIRER, S. NÖRSETT, AND G. WANNER, *Solving Ordinary Differential Equations I-II*, SCM 8, Springer, 1987.
- [17] W. HENSHAW, H.-O. KREISS, AND J. YSTRÖM, *Numerical Experiments on the Interaction Between the Large- and Small-Scale Motions of the Navier–Stokes Equations*, Multiscale Modeling and Simulation, 1 (2003), pp. 119–149.
- [18] J. M. HYMAN AND B. NICOLAENKO, *The Kuramoto-Sivashinsky equation: A bridge between PDE’s and dynamical systems*, Physica D, 18 (1986), pp. 113–126.
- [19] J. M. HYMAN, B. NICOLAENKO, AND S. ZALESKI, *Order and complexity in the Kuramoto-Sivashinsky model of weakly turbulent interfaces*, Physica D, 23 (1986), pp. 265–292.
- [20] P. KLOEDEN AND E. PLATEN, *Numerical solution of stochastic differential equations*, Springer, NY, 1999.
- [21] Y. KURAMOTO AND T. TSUZUKI, *On the formation of dissipative structures in reaction-diffusion systems*, Prog. Theor. Phys., 54 (1975), pp. 687–699.
- [22] J. LAMBERT, *Numerical methods for ordinary differential systems*, John Wiley, NY, 1991.
- [23] E. LEHMANN, *Theory of Point Estimation*, Wiley, NY, 1983.
- [24] K. LIN, *Random Perturbations of SRB Measures and Numerical Studies of Chaotic Dynamics*, PhD thesis, Department of Mathematics, University of California Berkeley, 2003.
- [25] A. MAJDA, I. TIMOFEYEV, AND E. V. ELJNDEN, *A Mathematical Framework for Stochastic Climate Models*, Comm. Pure Appl. Math., LIV (2001), pp. 891–974.
- [26] ———, *A priori tests of a stochastic mode reduction strategy*, Physica D, 170 (2002), pp. 206–252.
- [27] A. MCCOY, *A Numerical Study of Turbulent Diffusion*, PhD thesis, Department of Mathematics, University of California Berkeley, 1975.
- [28] G. MCLACHLAN AND T. KRISHNAN, *The EM algorithm and extensions*, John Wiley, NY, 1997.
- [29] H. MORI, *Transport, collective motion, and Brownian motion*, Prog. Theor. Phys., 33 (1965), pp. 423–450.
- [30] S. NORDHOLM AND R. ZWANZIG, *A systematic derivation of exact generalized Brownian motion theory*, J. Stat. Phys., 13 (1975), pp. 347–371.
- [31] D. ORMONEIT AND V. TRESP, *Averaging, maximum penalized likelihood and bayesian estimation for improving Gaussian mixture probability density estimates*, IEEE Trans. Neural Networks, 9 (1998).
- [32] M. PERRONE AND L. COOPER, *When networks disagree: Ensemble methods for hybrid neural networks*, in Artificial Neural Networks for Speech and Vision, R. Mammone, ed., Chapman and Hall, 1993, pp. 126–142.
- [33] M. ROST AND J. KRUG, *A particle model for the Kuramoto-Sivashinsky equation*, Physica D, 88 (1995), pp. 1–13.
- [34] G. SIVASHINSKY, *Nonlinear analysis of hydrodynamic instability in laminar flames, Part I. Derivation of basic equations*, Acta Astronautica, 4 (1977), pp. 1177–1206.
- [35] P. STINIS, *Optimal prediction for the Kuramoto-Sivashinsky equation*, PhD thesis, Department of Applied Physics and Applied Mathematics, Columbia University, New York, 2003.
- [36] S. TOH, *Statistical model with localized structures describing the spatio-temporal chaos of Kuramoto-Sivashinsky equation*, J. Phys. Soc. Japan, 56 (1987), pp. 949–962.
- [37] J. VERBEEK, N. VLASSIS, AND B. KROSE, *Efficient greedy learning of Gaussian mixtures*, Neural computation, 15 (2003), pp. 451–461.
- [38] R. L. WITTENBERG AND P. HOLMES, *Scale and space localization in the Kuramoto-Sivashinsky equation*, Chaos, 9 (1999), pp. 452–465.
- [39] A. YAGLOM, *An Introduction to the Theory of Stationary Random Functions*, Prentice-Hall, NJ, 1962.

- [40] V. YAKHOT, *Large scale properties of unstable systems governed by the Kuramoto-Sivashinsky equation*, Phys. Rev. A, 24 (1981), pp. 31–66.
- [41] R. ZWANZIG, *Nonlinear generalized Langevin equations*, J. Stat. Phys., 9 (1973), pp. 215–220.